Carbohydrate Polymers 95 (2013) 214–219

Contents lists available at SciVerse ScienceDirect

Carbohydrate Polymers

journal homepage: www.elsevier.com/locate/carbpol

Facile synthesis of tunable silver nanostructures for antibacterial application using cellulose nanocrystals

Rui Xiong, Canhui Lu, Wei Zhang, Zehang Zhou, Xinxing Zhang*

State Key Laboratory of Polymer Materials Engineering, Polymer Research Institute of Sichuan University, Chengdu 610065, China

ARTICLE INFO

Article history:
Received 8 January 2013
Received in revised form 19 February 2013
Accepted 28 February 2013
Available online 7 March 2013

Keywords:
Cellulose nanocrystals
Silver nanostructure
Antibacterial activity
Shape control
Environmentally friendly synthesis

ABSTRACT

In this study, we report a facile and environmentally friendly strategy for synthesis of well dispersed and stable silver nanostructures using cellulose nanocrystals in aqueous solution without employing any other reductants, capping or dispersing agents. Importantly, it is feasible to adjust the morphology of the silver nanostructures by varying the precursor $AgNO_3$ concentration. Silver nanospheres were formed when the $AgNO_3$ concentration was 0.4 mM, while the dendritic nanostructures predominated when the $AgNO_3$ concentration was increased to 250 mM. The antibacterial activity of the two different silver nanostructures against *Escherichia coli* and *Staphylococcus aureus* was characterized. Dendritic nanostructure showed a better antibacterial activity than that of silver nanosphere. The approach presented in this paper offers a very promising route to noble metal nanoparticles using renewable reducing agents.

1. Introduction

Noble metal nanoparticles, especially silver nanoparticles (Ag NPs) have attracted considerable attention due to their potential applications as electronic, optical, sensing, catalytic and importantly antibacterial materials. Silver has been utilized in antibacterial applications for thousands of years due to their broad-spectrum antimicrobial activities and high toxicity to different type of microorganisms (Kamel, 2012; Nassar & Youssef, 2012). However, among the conventional preparative methods, most of the reducing and stabilizing reagents used for the synthesis of Ag NPs are not environmentally benign. In view of the awareness toward green chemistry and sustainable strategy, the development of a simple and environment-friendly method for the synthesis of Ag NPs is necessary.

Biological synthesis of metal NPs using microorganisms, enzymes, and carbohydrate polymers have been suggested as possible eco-friendly alternatives to conventional petrochemical reductants-based methods (Iravani, 2011; Shaligram et al., 2009). A number of researchers have described the synthesis of various metal NPs using carbohydrate polymers, such as leaf broth (Shankar, Ahmad, Pasrichaa, & Sastry, 2003), hydroxypropyl starch (Hebeish et al., 2011), hydroxypropyl cellulose (Abdel-Halim & Al-Deyab, 2011) and bacterial cellulose (Yang, Xie, Deng, Bian, & Hong, 2012). Using renewable carbohydrate- or cellulose-based materials for the synthesis of NPs can be advantageous over microorganisms process because it eliminates the elaborate process of maintaining cell cultures and can also be suitably scaled up for large-scale NPs synthesis (Song, Jang, & Kim, 2009). Moreover, NPs produced by carbohydrate- or cellulose-based materials are more stable and the rate of synthesis is faster than that in the case of microorganisms (Iravani, 2011).

Cellulose nanocrystals (CNs), which can be isolated from a variety of natural sources such as cotton, tunicate, bacteria and wood pulp, has emerged as a new class of renewable carbohydrate polymers owing to its high stiffness, low density, well-defined size and morphology, controlled surface chemistry, environmental sustainability and anticipated low cost (Lam, Hrapovic, Majid, Chong, & Luong, 2012). The electron-rich feature of hydroxyl and sulfate ester groups on its surface endow CNs a good colloidal stability in water, which makes it well suitable for the preparation of metal NPs (Benaissi, Johnson, Walsh, & Thielemans, 2010; Hirai, Nakao, & Toshima, 1979; Lin et al., 2011). However, to date, the use of CNs in the biosynthesis of metal NPs is very limited. A small number of reports (Cirtiu, Dunlop-Briere, & Moores, 2011; Lam et al., 2012; Shin, Bae, Arey, & Exarhos, 2008) describe the formation of metal NPs using CNs as a stabilizing template, which inevitably involved the use of a chemical reducing agent. Recently, synthesis of platinum NPs using CNs as a reducing agent was reported by Benaissi et al. (2010). However, their results indicated that the reaction only proceeds when the water is in contact with supercritical carbon dioxide. The strict reaction condition hindered the

* Corresponding author. Tel.: +86 28 85460607; fax: +86 28 85402465.
E-mail address: xxzwwh@scu.edu.cn (X. Zhang).

0144-8617/$ – see front matter © 2013 Elsevier Ltd. All rights reserved.
http://dx.doi.org/10.1016/j.carbpol.2013.02.077

large-scale application of this approach. To the best knowledge of the authors, no reports on the facile synthesis of metal NPs using CNs as reductant and stabilizer under mild conditions have been published.

Herein we present the successful synthesis of Ag NPs using CNs in aqueous solution without employing any other reductants, capping or dispersing agents under mild conditions. Furthermore, it is feasible to adjust the morphology of the Ag nanostructures by varying the precursor $AgNO_3$ concentration. We report for the first time that the dendritic Ag nanostructures can be obtained using CNs as a reducing agent. The antibacterial activity of Ag NPs with different nanostructures against *Escherichia coli* and *Staphylococcus aureus* was investigated. The green and environmentally benign approach developed in this paper offers a very promising route to the synthesis of other metal NPs, especially those to be used for antibacterial applications.

2. Experimental

2.1. Materials

All chemical materials and solvents used in the experiments were analytical grade reagents, and were used without further purification. Waste cotton fabrics were obtained commercially from the surplus of textile industries. Silver nitrate ($AgNO_3$), hydrochloric acid, nitric acid and sulfuric acid were purchased from Kelong Chemical Regent Co., Ltd. (Chengdu, China). All solutions were prepared with deionized water.

2.2. Preparation of CNs

The CNs was obtained by acid hydrolyzing the microcrystalline cellulose (MCC). The method of preparing MCC has been reported in our previous work (Xiong, Zhang, Tian, Zhou, & Lu, 2012), and the procedure of preparing CNs is based on the report of Bondeson, Mathew, and Oksman, 2006). The MCC and sulfuric acid (64 wt%) suspension were heated with stirring at 45 °C for 130 min. The suspensions were then washed with deionized water using repeated centrifuge cycles (10 min at 12,000 rpm for a cycle). The last wash was conducted using dialysis with deionized water until the wash water maintained a constant pH.

2.3. Hydrothermal synthesis of silver nanosphere and dendritic nanostructure

In a typical experiment, the desired amount of the metal precursor, $AgNO_3$ (0.4 and 250 mM), was added to 30 ml aq. 0.1 wt% CNs suspension in a hydrothermal synthesis reaction kettle for 12 h at 100 °C. Then the suspensions were washed with deionized water using repeated centrifuge cycles (10 min at 12,000 rpm for a cycle) to remove the unreacted $AgNO_3$.

2.4. Characterization

The transmission electron microscopy (TEM, JEOL JEM-100CX, Japan) and atomic force microscopy (AFM, Nanoscope Multimode & Exoplore, Vecco Instruments Inc., USA) was carried out to observe the morphology of the obtained CNs. The morphology and structure of the obtained CNs and Ag nanostructures were measured by TEM (JEOL JEM-100CX, Japan), high resolution transmission electron microscopy (HRTEM), selected area electron diffraction (SAED) and energy dispersive X-ray spectroscopy (EDS). The particle sizes of the Ag NPs were measured using ImageJ software. In order to measure the particle size accurately, those uncovered particles by the cellulose microfibrils were chose for measurement, and at least 100 particles of the sample from different TEM images were analyzed. The UV–vis spectra were taken at room temperature on a Mapada UV-1800 spectrophotometer using a quartz cuvette with an optical path of 1 cm. The XRD patterns were collected on a Philips Analytical X'Pert X-diffractometer (Philips Co., Netherlands), using Cu-Kα radiation ($k = 0.1540$ nm) at an accelerating voltage of 40 kV and the current of 40 mA. The data were collected from $2\theta = 35–80°$. The contents of Ag in the nanocomposites were determined by atomic absorption spectroscopy (AAS).

2.5. Antibacterial assays

E. coli (ATCC 25922) and *S. aureus* (ATCC 6538) were used for antibacterial activity assessments by using the minimum inhibitory concentrations (MIC) method. The MICs were quantified using a broth microdilution method according to National committee for clinical laboratory (NCCLS). For the tests of the ability of nanohybrids to inhibit bacterial growth, concentrated aqueous dispersions of CNs/Ag nanosphere and CNs/Ag dendritic nanostructre hybrids at concentrations of 1000 mg/L were prepared. For determination of the MIC values, the concentrations of CNs/Ag nanosphere and CNs/Ag dendritic nanostructre hybrids were adjusted by 2–128 times dilution using geometrical progression. The testing of CNs/Ag nanosphere and CNs/Ag dendritic nanostructre hybrids and determination of MIC values were independently repeated at least twice.

3. Results and discussion

3.1. Morphological observation of CNs

Fig. 1a shows a TEM image of CNs, which has been isolated from waste cotton fabrics by acid hydrolysis. CNs suspension contains rod-like crystalline celluloses with 10–20 nm in diameter and 100–200 nm in length. In order to further observe the morphology of the CNs, AFM analysis was carried out. Fig. 1b shows the AFM micrograph of the obtained CNs in suspension. Aggregations are observed in CNs, which might be ascribed to the water evaporation. Meanwhile, some isolated individual particles are clearly observed especially in the AFM image (Fig. 1b). The individual particles clearly demonstrate that the CNs indeed are rod-like particles. The dimension of the CNs corresponds well with the TEM images. The CNs suspension has a good stability, because the incorporation of sulfate groups on the cellulose surface creates a strong electrostatic repulsion between the anionic sulfate ester groups at the surface. (Klemm et al., 2011). Therefore, CNs exposed a larger specific surface area, which is expected to possess a better reducing and stabilizing ability.

3.2. UV–vis analysis

Fig. 2a shows the digital camera picture of the CNs, CNs/Ag nanospheres and CNs/Ag dendritic nanostructure suspensions. It is well known that Ag NPs exhibit yellow colors, these colors arising due to excitation of surface plasmon vibrations in the Ag NPs (Shankar, Rai, Ahmad, & Sastry, 2004). Both the CNs/Ag nanospheres and dendritic nanostructure suspension shows a good stability due to stabilization of the CNs. Fig. 2b shows the UV–vis absorption spectrum of Ag nanospheres and Ag dendritic nanostructure, which is obtained by dispersing the CNs/Ag particles in water under sonication. The spectrum of Ag nanospheres shows the characteristic surface plasmon resonance (SPR) absorption band at 426 nm. In contrast, the SPR adsorption of Ag dendritic nanostructure is at 500 nm. It is consistent with the SPR absorption band of the Ag NPs in literature (Song & Kim, 2009), which indicates

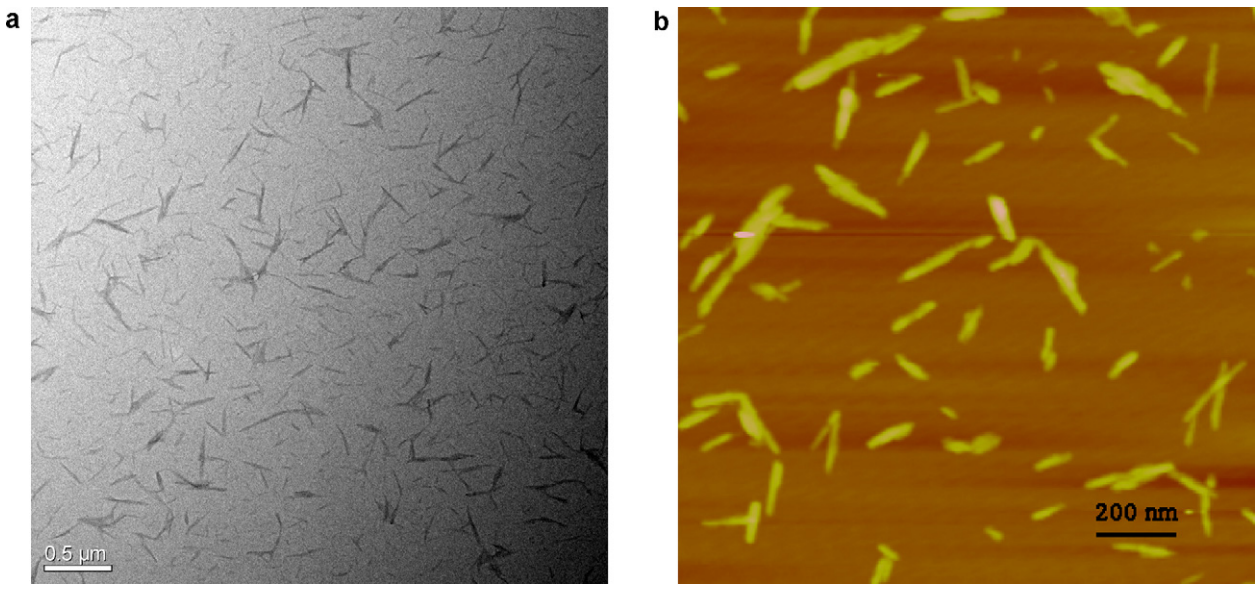

Fig. 1. Morphology of CNs derived from waste cotton fabrics. (a) TEM and (b) AFM.

the successful preparation of Ag NPs. The absorption band of Ag nanospheres is symmetrical and narrow, which suggests that the size of the nanospheres is uniform. The absorption band broadening and shifts from 426 to 450 nm with the increasing of $AgNO_3$ concentration from 0.4 to 250 mM, indicating the polydispersity and increase of the particle size of silver.

3.3. XRD analysis

Fig. 3 shows the X-ray diffraction pattern of Ag nanospheres and Ag dendritic nanostructure. Two main peaks at 38.2 and 44.4° in Ag dendritic nanostructure curve are assigned to (1 1 1) and (2 0 0) planes of cubic silver. However, only a small peak with a low intensity at 38.2° of the silver crystal in Ag nanospheres was observed, which resulted from the small amount of silver in the CNs/Ag nanospheres. This is also in a full accordance with the result of AAS (Table 1). The Ag content of CNs/Ag nanospheres and CNs/Ag dendritic nanostructure is 6.6 and 52.6%, respectively, which resulted from the different amount of $AgNO_3$ used in the synthesis. XRD

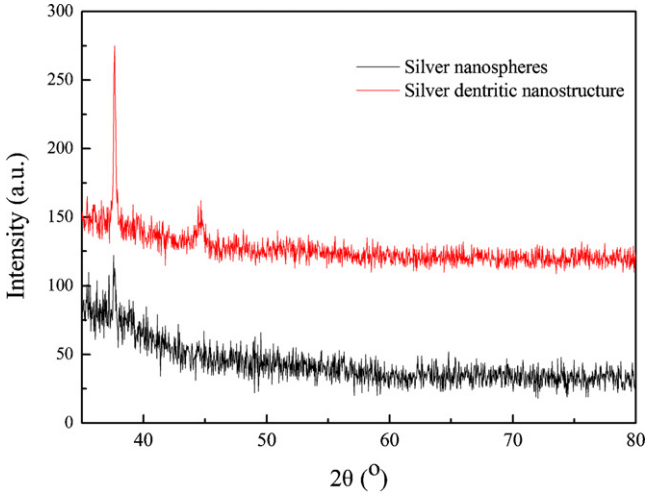

Fig. 3. XRD diagram of Ag nanospheres and Ag dendritic nanostructure.

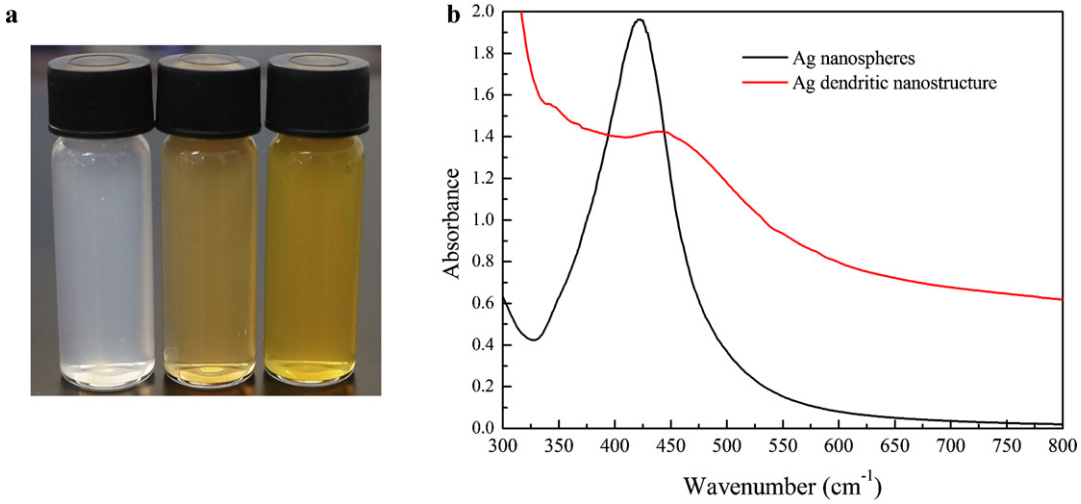

Fig. 2. (a) Digital camera picture of CNs (left), CNs/Ag nanospheres (middle) and CNs/Ag dendritic nanostructure (right), (b) UV–vis spectrums of Ag nanospheres and Ag dendritic nanostructure.

Table 1
The contents of Ag in the hybrids determined by atomic absorption spectroscopy (AAS).

Samples	Ag contents (wt%)
CNs/Ag nanoshperes	6.6
CNs/Ag dendritic nanostructure	52.6

pattern clearly illustrates that the Ag NPs formed in this study are crystalline in nature.

3.4. TEM and SAED analysis

Fig. 4a shows the TEM image of typical Ag nanospheres that was prepared when the concentration of $AgNO_3$ was 0.4 mM. These particles are generally spherical in shape. The Ag nanospheres show good dispersion and stability, because CNs acts not only a reductant but also a stabilizer (Song & Kim, 2009). From the inserted particle size distribution diagram of the Ag nanospheres (up-right in Fig. 4a), it can be observed that the most distributed dimension is in the range of 1–10 nm. The image (up-left in Fig. 4a) shows the selected area SAED pattern recorded of the Ag nanospheres. The ring-like diffraction pattern indicates that the bunch of Ag NPs is polycrystalline character. Fig. 4b shows the HRTEM images of an individual Ag nanosphere. It exhibits clear lattice fringes of ~0.23 nm, which is attributed to the (1 1 1) plane of fcc Ag. This result indicates that the individual Ag nanosphere is a single crystal.

What is more interesting is that with the concentration of $AgNO_3$ increased to 250 mM, there is an apparent different Ag dendritic nanostructure of fairly high density in the ensembles. Different from previously reported cases (Cao et al., 2005; Parfenov, Gryczynski, Malicka, Geddes, & Lakowicz, 2003; Peng, Dong, Deng, & Li, 2002), the "leaves" of this dendritic nanostructure in our study consist of many single tabular crystals instead of aggregated simple nanospheres, and these "leaves" resemble those in natural trees. The Ag dendritic nanostructure is shown in Fig. 5a, which exhibits a single morphology with many branches. The individual dendrite length is about 5–10 μm. The inserted image (up-right Fig. 5a) is the SEAD pattern of the dendritic structure, indicating a single crystal character. This point is further proved by the corresponding HRTEM (Fig. 5b). The HRTEM in Fig. 5b shows all the lattice planes is about 0.23 nm, which is nearly consistent with the (1 1 1) plane of fcc Ag phase, indicating that the growth direction of the dendritic silver is preferential in the [1 1 1] direction.

3.5. STEM and EDS analysis

High-angle annular dark field scanning TEM (HAADF/STEM) is a powerful tool for the characterization of nanostructured materials. Using HAADF/STEM, the Ag dendritic nanostructure stands out clearly (Fig. 6a). We further examined the chemical composition of the dendritic nanostructure by HAADF/STEM energy-dispersive X-ray spectroscopy (EDS). Strong peaks of the element Ag are observed in the EDS spectra of the selected area (Fig. 6b), confirming the formation of dendrite Ag nanostructure. The peaks of the element Cu are from the copper grid.

The presence of large density of the same structure of Ag dendritic nanostructure at a high silver ion concentration and Ag nanospheres at a low ion concentration suggests that diffusion of Ag nanocrystal precursors plays an important role in the formation of the Ag nanostructures. These results indicate that Ag dendritic nanostructure with well defined morphology and crystalline structure could be realized by controlling the $AgNO_3$ concentration in the solution.

3.6. Antibacterial testing

Antibacterial activities of the synthesized CNs/Ag nanosphere and CNs/Ag dendritic nanostructre were investigated by using the standard microdilution method, determining MIC of the CNs/Ag hybrid against *E. coli* and *S. aureus*. The ability of the hybrid to inhibit the growth of the tested strains is shown in Fig. 7. From the MIC values, it is evident that both hybrids significantly inhibited the growth of the tested bacterial strains. On the contrary, CNs does not show any antibacterial activity for both the tested strains at the highest tested concentration (1000 mg/L). This result proves that the antibacterial activities of the hybrid are owing to the silver particles loaded on the CNs. In Fig. 7a, the mutual comparison of both hybrid revealed that the slightly lower MIC values of CNs/Ag dendritic hybrid can be a result of a higher concentration of silver in the nanohybrids. In order to assess the antibacterial activities of the Ag NPs with different shape, MIC value

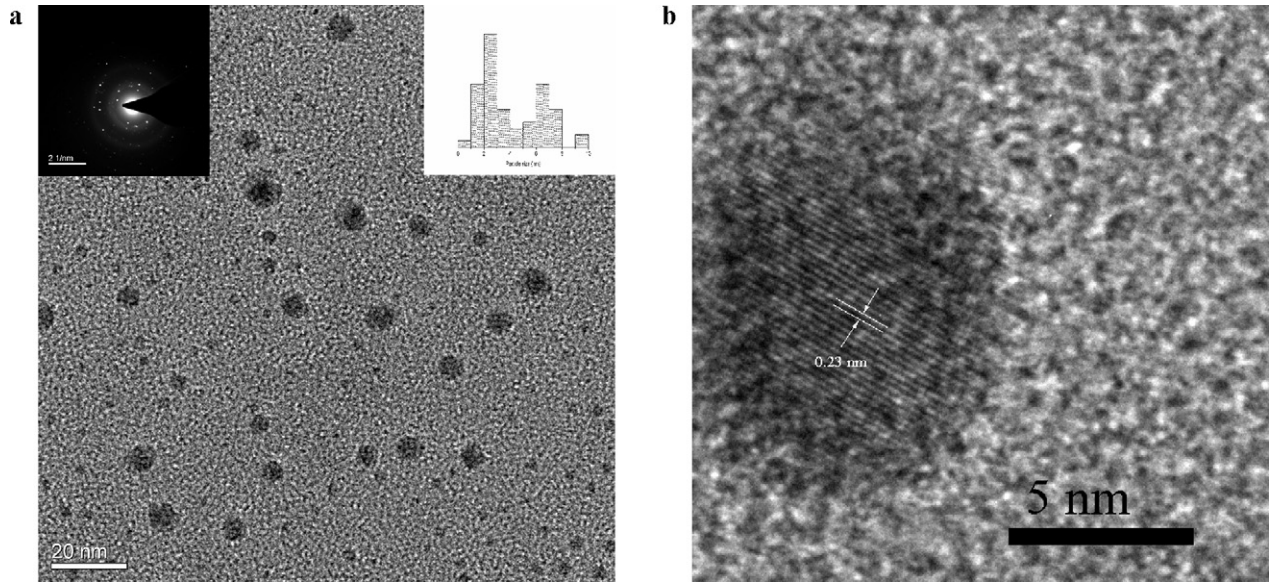

Fig. 4. Characterization of Ag nanospheres formed with 0.4 mM $AgNO_3$. (a) TEM image of Ag nanospheres inserted particle size distribution and SAED pattern. (b) HRTEM images of the Ag NPs found, ranging from 4 to 5 nm in size and possessing single crystal character.

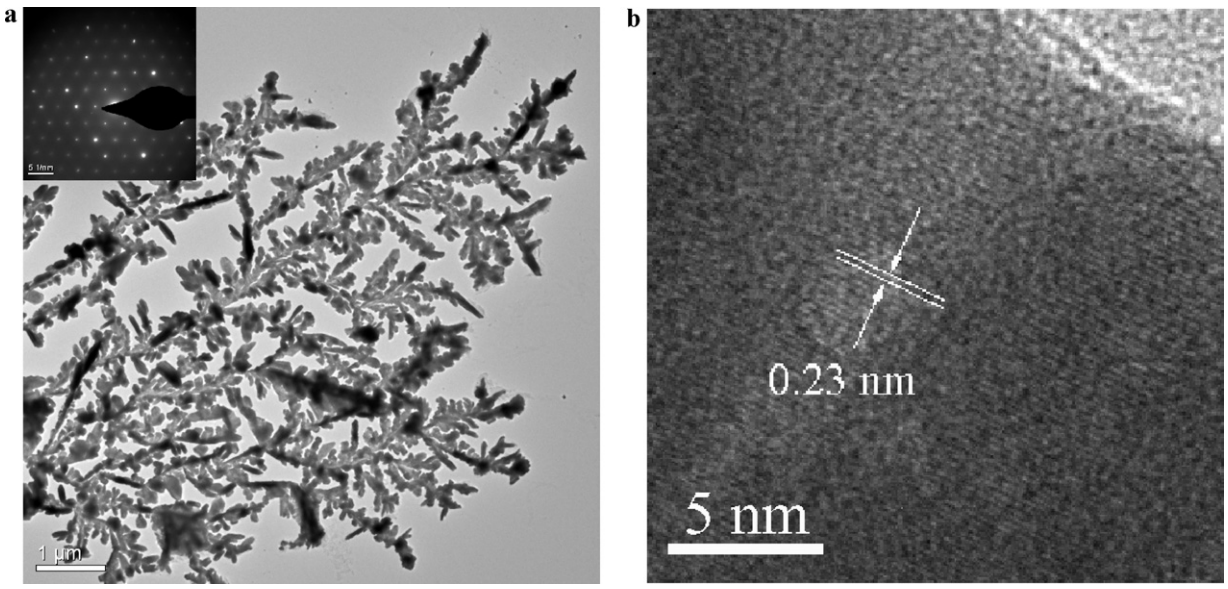

Fig. 5. Characterization of Ag dendritic nanostructures formed with 250 mM $AgNO_3$. (a) TEM image of Ag dentritic nanostructure inserted SAED pattern. (b) HRTEM of a branch.

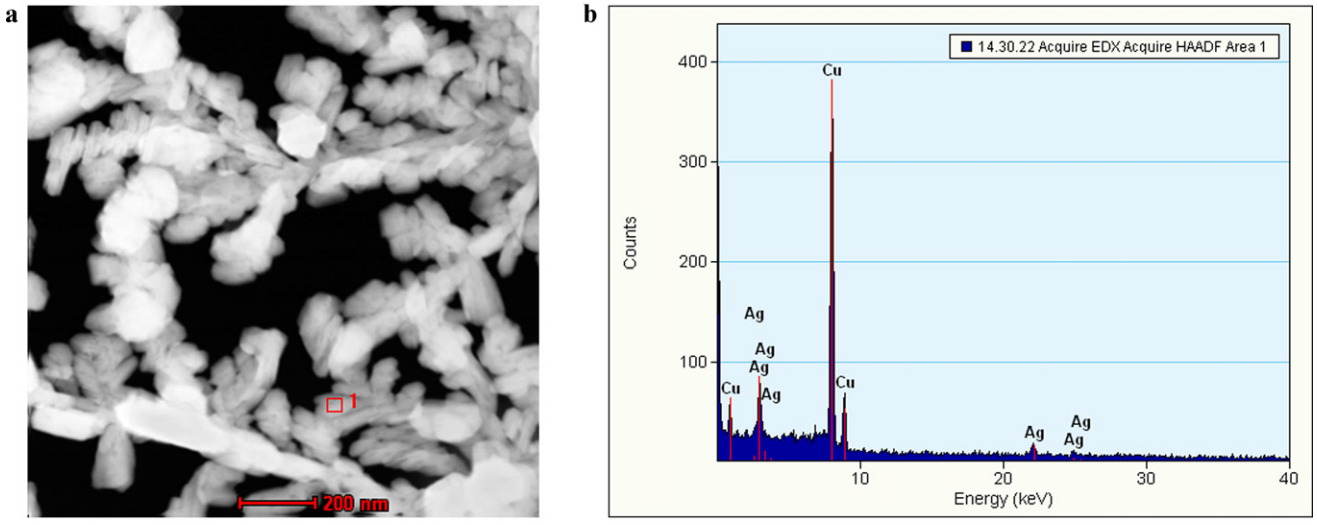

Fig. 6. (a) HAADF/STEM image and (b) EDS spectra of Ag dendritic nanostructures.

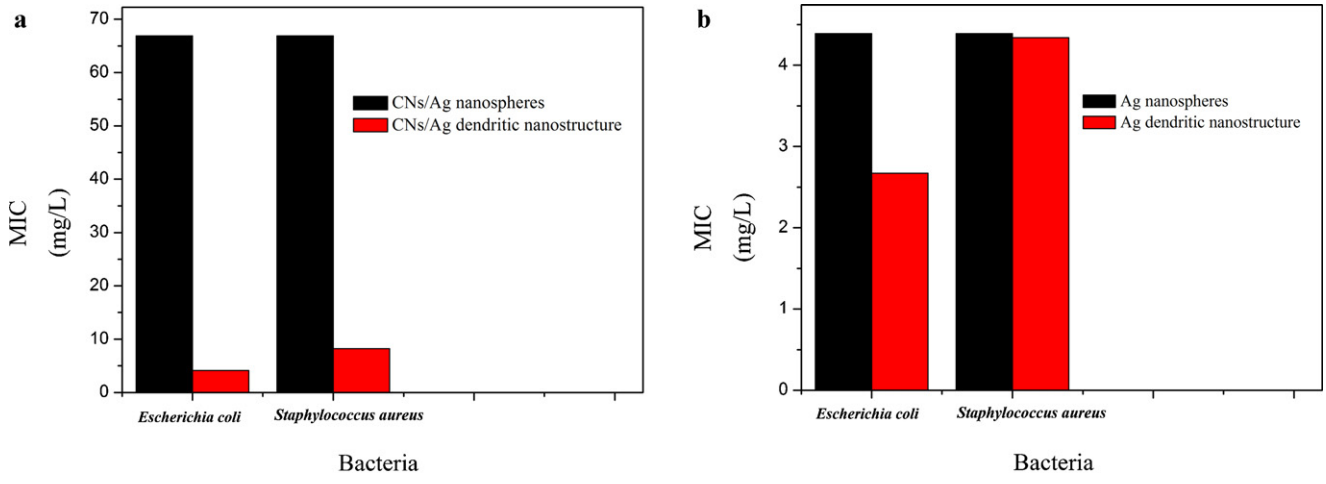

Fig. 7. (a) Minimum inhibitory concentrations (MIC) and (b) Ag-related MIC values of CNs/Ag nanospheres and CNs/Ag dendritic nanostructure determined against *Escherichia coli* and *Staphylococcus aureus*.

recalculated exclusively to Ag content in the respective hybrid (Fig. 7b). It was found that MIC of CNs/Ag dendritic nanostructure is also lower than that of CNs/Ag nanosphere. Moreover, the MIC value of CNs/Ag nanospheres against *S. aureus* was even found to be twice as much as that of CNs/Ag dendritic nanostructure. Therefore, it turns out that the antibacterial activity of Ag dendritic nanostructure is better than that of Ag nanospheres in the hybrid, which might be ascribed to its complex self-assemble hierarchical repeated structure. It should be emphasized that the antibacterial activity of the CNs/Ag hybrid prepared in this study is even comparable to those of colloidal silver dispersions (Panáček et al., 2006). The CNs/Ag hybrid with high antibacterial performance which could be facile prepared has a great potential to be used in various antibacterial applications, such as health care and food packages.

4. Conclusion

In conclusion, we have demonstrated that CNs could be used to facilely synthesize of well dispersed and stable Ag NPs with different nanostructures. The CNs covered with extensive hydroxyl groups served as both the reducing and stabilizing agent for the formation of Ag NPs. The concentration of $AgNO_3$ played an important role in the adjustment of Ag nanostructures. The CNs/Ag nanohybrids exhibit an excellent antibacterial performance comparable to those of colloidal silver dispersions. The facile biosynthesis approach could also be extended to the synthesis of other metal-contained cellulose nanohybrids, and this type of biocompatible antibacterial material is proposed to have promising potential in biomedical, cosmetics, health care and many other related fields.

Acknowledgements

The authors would like to thank the National Science Foundation of China (51203105) and National High Technology Research and Development Program (863 Program, SS2012AA062613) for financial support.

References

Abdel-Halim, E. S., & Al-Deyab, S. S. (2011). Utilization of hydroxypropyl cellulose for green and efficient synthesis of silver nanoparticles. *Carbohydrate Polymers*, *86*, 1615–1622.

Benaissi, K., Johnson, L., Walsh, D. A., & Thielemans, W. (2010). Synthesis of platinum nanoparticles using cellulosic reducing agents. *Green Chemistry*, *12*, 220–222.

Bondeson, D., Mathew, A., & Oksman, K. (2006). Optimization of the isolation of nanocrystals from microcrystalline cellulose by acid hydrolysis. *Cellulose*, *13*, 171–180.

Cao, M. H., Liu, T. F., Gao, S., Sun, G., Wu, X. L., Hu, C. W., et al. (2005). Single-crystal dendritic micro-pines of magnetic α-Fe_2O_3: Large-scale synthesis, formation mechanism, and properties. *Angewandte Chemie-International Edition*, *44*, 4197–4201.

Cirtiu, C. M., Dunlop-Briere, A. F., & Moores, A. (2011). Cellulose nanocrystallites as an efficient support for nanoparticles of palladium: Application for catalytic hydrogenation and Heck coupling under mild condition. *Green Chemistry*, *13*, 288–291.

Hebeish, A., El-Naggara, M. E., Fouda, M. M. G., Ramadan, M. A., Al-Deyab, S. S., & El-Rafie, M. H. (2011). Highly effective antibacterial textiles containing green synthesized silver nanoparticles. *Carbohydrate Polymers*, *86*, 936–940.

Hirai, H., Nakao, Y., & Toshima, N. (1979). Preparation of colloidal transition metals in polymers by reduction with alcohols or ethers. *Journal of Macromolecular Science A*, *13*, 727–750.

Iravani, S. (2011). Green synthesis of metal nanoparticles using plants. *Green Chemistry*, *13*, 2638–2650.

Kamel, S. (2012). Rapid synthesis of antimicrobial paper under microwave irradiation. *Carbohydrate Polymers*, *90*, 1538–1542.

Klemm, D., Kramer, F., Moritz, S., Lindstrom, T., Ankerfors, M., Gray, D., et al. (2011). Nanocelluloses: A new family of nature-based materials. *Angewandte Chemie-International Edition*, *50*, 5438–5466.

Lam, E., Hrapovic, S., Majid, E., Chong, J. H., & Luong, J. H. T. (2012). Catalysis using gold nanoparticles decorated on nanocrystalline cellulose. *Nanoscale*, *4*, 997–1002.

Lin, X., Wu, M., Wu, D., Kuga, S., Endo, T., & Huang, Y. (2011). Platinum nanoparticles using wood nanomaterials: eco-friendly synthesis, shape control and catalytic activity for *p*-nitrophenol reduction. *Green Chemistry*, *13*, 283–287.

Nassar, M. A., & Youssef, A. M. (2012). Mechanical and antibacterial properties of recycled carton paper coated by PS/Ag nanocomposites for packaging. *Carbohydrate Polymers*, *89*, 269–274.

Panáček, A., Kvítek, L., Prucek, R., Kolář, M., Večerová, R., Pizúrová, N., et al. (2006). Silver colloid nanoparticles: Synthesis, characterization, and their antibacterial activity. *The Journal of Physical Chemistry B*, *110*, 16248–16253.

Parfenov, A., Gryczynski, I., Malicka, J., Geddes, C. D., & Lakowicz, J. R. (2003). Enhanced fluorescence from fluorophores on fractal silver surfaces. *The Journal of Physical Chemistry B*, *107*, 8829–8833.

Peng, Q., Dong, Y. J., Deng, Z. X., & Li, Y. D. (2002). Selective synthesis and characterization of CdSe nanorods and fractal nanocrystals. *Inorganic Chemistry*, *41*, 5249–5254.

Shaligram, N. N., Bule, M., Bhambure, R., Singhal, R. S., Singh, S. K., Szakacs, G., et al. (2009). Biosynthesis of silver nanoparticles using aqueous extract from the compactin producing fungal strain. *Process Biochemistry*, *44*, 939–943.

Shankar, S. S., Ahmad, A., Pasrichaa, R., & Sastry, M. (2003). Bioreduction of chloroaurate ions by geranium leaves and its endophytic fungus yields gold nanoparticles of different shapes. *Journal of Materials Chemistry*, *13*, 1822–1826.

Shankar, S. S., Rai, A., Ahmad, A., & Sastry, M. (2004). Rapid synthesis of Au, Ag, and bimetallic Au core Ag shell nanoparticles using neem (*Azadirachta indica*) leaf broth. *Journal of Colloid and Interface Science*, *275*, 496–502.

Shin, Y., Bae, I., Arey, B. W., & Exarhos, G. J. (2008). Facile stabilization of gold-silver alloy nanoparticles on cellulose nanocrystal. *The Journal of Physical Chemistry C*, *112*, 4844–4848.

Song, J. Y., & Kim, B. S. (2009). Rapid biological synthesis of silver nanoparticles using plant leaf extracts. *Bioprocess and Biosystems Engineering*, *32*, 79–84.

Song, J. Y., Jang, H. K., & Kim, B. S. (2009). Biological synthesis of gold nanoparticles using *Magnolia kobus* and *Diopyros kaki* leaf extracts. *Process Biochemistry*, *44*, 1133–1138.

Xiong, R., Zhang, X., Tian, D., Zhou, Z., & Lu, C. (2012). Comparing microcrystalline with spherical nanocrystalline cellulose from waste cotton fabrics. *Cellulose*, *4*, 1189–1198.

Yang, G., Xie, J., Deng, Y., Bian, Y., & Hong, F. (2012). Hydrothermal synthesis of bacterial cellulose/AgNPs composite: A green route for antibacterial application. *Carbohydrate Polymers*, *87*, 2482–2487.